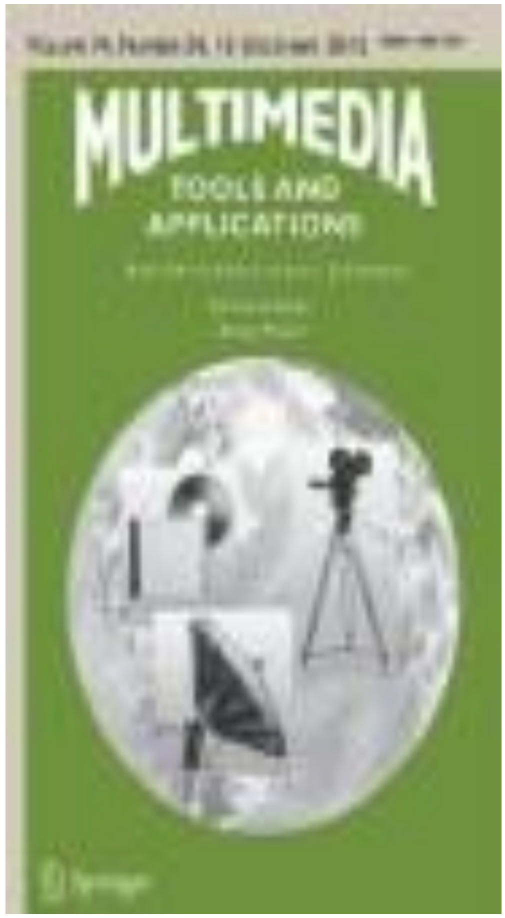
MULTIMEDIA
TOOLS AND
APPLICATIONS
Springer

Aims and scope

Multimedia Tools and Applications publishes original research articles on multimedia development and system support tools, and case studies of multimedia applications. Experimental and survey articles are appropriate for the journal. The journal is intended for academics, practitioners, scientists and engineers who are involved in multimedia system research, design and applications. All papers are peer reviewed.

Editors

[Appearance-based bidirectional representation for palmprint recognition]

Jinrong Cui, Jiajun Wen & Zizhu Fan

OriginalPaper | Published: 14 February 2014

Pages: 10989 - 11001

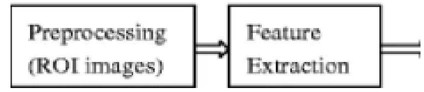

[Erratum to: Appearance-based bidirectional representation for palmprint recognition]

Jinrong Cui, Jiajun Wen & Zizhu Fan

Erratum | Published: 09 November 2015 | Pages: 11003 - 11005

[Use of symmetry in prediction-error field for lossless compression of 3D MRI images]

N. Karimi, S. Samavi ... S. Shirani

OriginalPaper | Published: 23 August 2014

Pages: 11007 - 11022

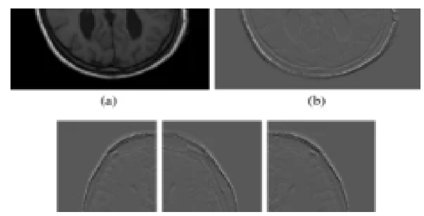

[A fast inter-prediction algorithm for HEVC based on temporal and spatial correlation]

Guoyun Zhong, Xiaohai He ... Yuan Li

OriginalPaper | Published: 01 August 2014

Pages: 11023 - 11043

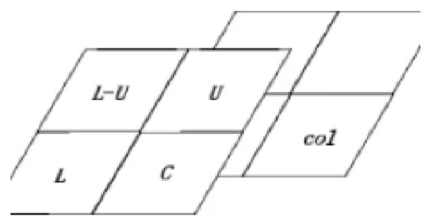

[Steganalysis of perturbed quantization steganography based on the enhanced histogram features](#)

Xiaofeng Song, Fenlin Liu ... Yi Zhang

OriginalPaper | Published: 06 September 2014

Pages: 11045 - 11071

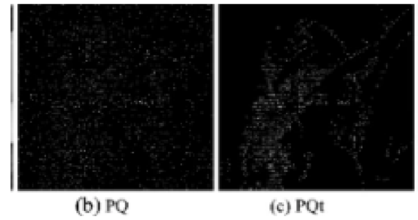

[A camera motion histogram descriptor for video shot classification](#)

Muhammad Abul Hasan, Min Xu ... Yi Wang

OriginalPaper | Published: 14 August 2014

Pages: 11073 - 11098

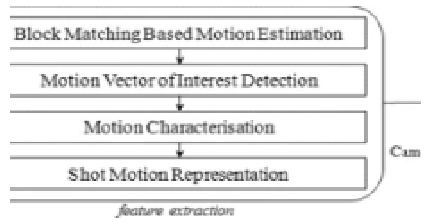

[Anomaly detection in compressed H.264/AVC video](#)

Sovan Biswas & R. Venkatesh Babu

OriginalPaper | Published: 28 August 2014

Pages: 11099 - 11115

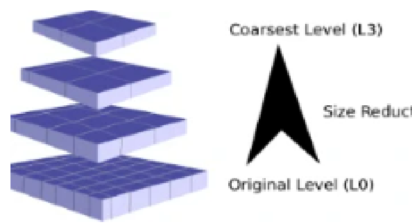

[An adaptive caching algorithm suitable for time-varying user accesses in VOD systems](#)

Qiang Ling, Lixiang Xu ... Yicheng Zhang

OriginalPaper | Published: 16 August 2014

Pages: 11117 - 11137

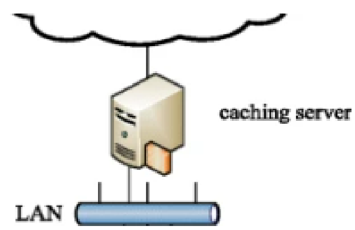

[Tree group based Wavelet Watermarking using Energy Modulation and Consistency Check (WW-EMCC) for digital images](#)

Min-Jen Tsai, Jin-Sheng Yin & Imam Yuadi

OriginalPaper | Published: 19 August 2014

Pages: 11139 - 11161

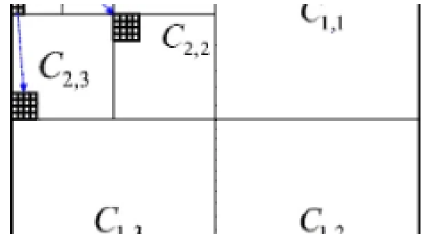

[Defining embedding distortion for motion vector-based video steganography](#)

Yuanzhi Yao, Weiming Zhang ... Xianfeng Zhao

OriginalPaper | Published: 03 September 2014

Pages: 11163 - 11186

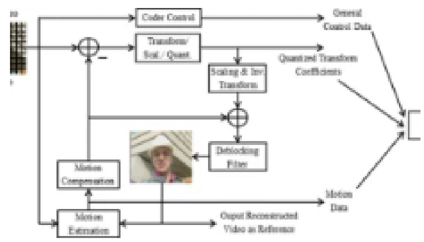

[Keyframe extraction in endoscopic video](#)

Klaus Schoeffmann, Manfred Del Fabro ... Jörg Keckstein

OriginalPaper | Published: 29 August 2014

Pages: 11187 - 11206

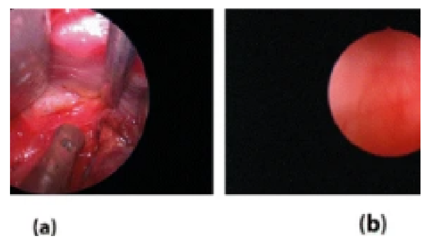

[3-D body joint-specific HMM-based approach for human activity recognition from stereo posture image sequence](#)

Md. Zia Uddin & Tae-Seong Kim

OriginalPaper | Published: 15 August 2014

Pages: 11207 - 11222

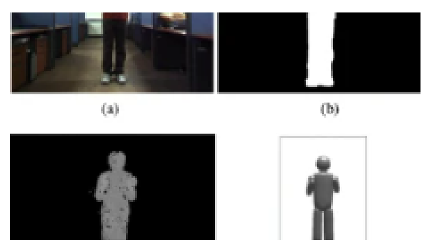

A multi-channel based illumination compensation mechanism for brightness invariant image retrieval

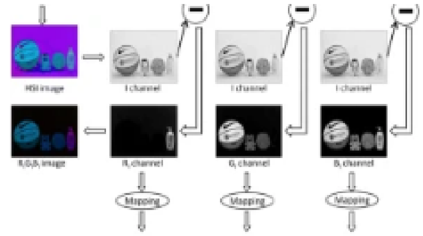

Shiv Ram Dubey, Satish Kumar Singh & Rajat Kumar Singh

OriginalPaper | Published: 14 August 2014

Pages: 11223 - 11253

A new algorithm of image compression and encryption based on spatiotemporal cross chaotic system

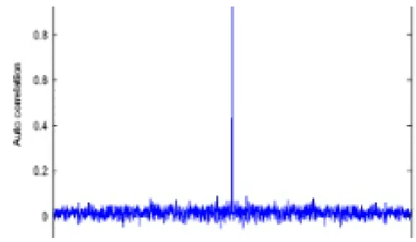

Miao Zhang & Xiaojun Tong

OriginalPaper | Published: 17 August 2014

Pages: 11255 - 11279

Regularized directional feature learning for face recognition

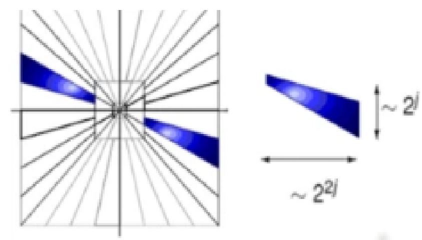

Mohamed Anouar Borgi, Maher El'Arbi ... Chokri Ben Amar

OriginalPaper | Published: 03 September 2014

Pages: 11281 - 11295

Online optimization for user-specific hybrid recommender systems

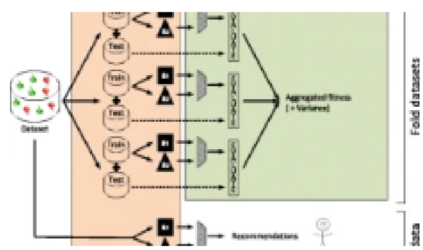

Simon Dooms, Toon De Pessemier & Luc Martens

OriginalPaper | Published: 29 August 2014

Pages: 11297 - 11329

[Assessment of female facial beauty based on anthropometric, non-permanent and acquisition characteristics]

Antitza Dantcheva & Jean-Luc Dugelay

OriginalPaper | Published: 09 September 2014

Pages: 11331 - 11355

Performance evaluation of new colour histogram-based interest point detectors

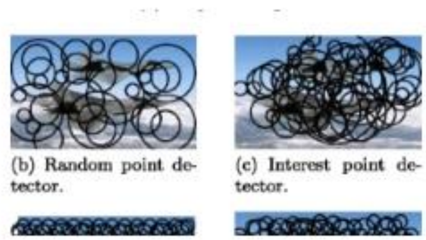

Taha H. Rassem & Bee Ee Khoo

OriginalPaper | Published: 09 September 2014

Pages: 11357 - 11398

Towards context-sensitive collaborative media recommender system

Mohammed F. Alhamid, Majdi Rawashdeh ... Abdulmotaleb El Saddik

OriginalPaper | Published: 03 September 2014

Pages: 11399 - 11428

An efficient steganographic framework based on dynamic blocking and genetic algorithm

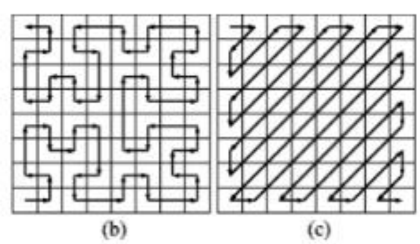

Mehran Iranpour & Mohammad Rahmati

OriginalPaper | Published: 14 September 2014

Pages: 11429 - 11450

[The credit card visual authentication scheme based on $GF(2^8)$ field](#)

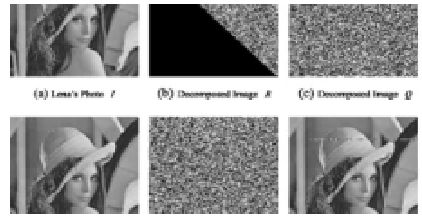

Feng Wang, Chin-Chen Chang & Wan-Li Lyu

OriginalPaper | Published: 16 September 2014

Pages: 11451 - 11465

[Color sensing and image processing-based automatic soybean plant foliar disease severity detection and estimation](#)

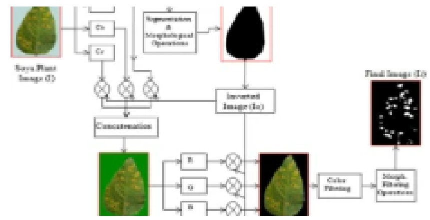

Sourabh Shrivastava, Satish Kumar Singh & Dhara Singh Hooda

OriginalPaper | Published: 19 September 2014

Pages: 11467 - 11484

[Removal of random-valued impulse noise by local statistics](#)

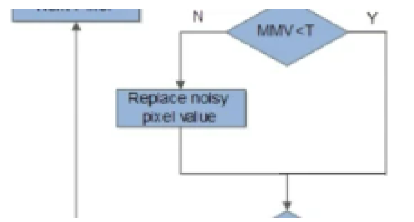

Hassan Dawood, Hussain Dawood & Ping Guo

OriginalPaper | Published: 28 September 2014

Pages: 11485 - 11498

[Learning human photo shooting patterns from large-scale community photo collections](#)

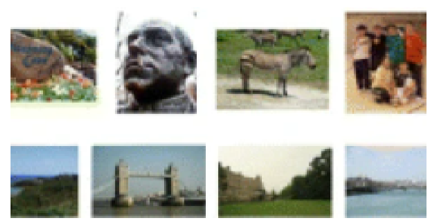

Yanpeng Cao & Kay O'Halloran

OriginalPaper | Published: 06 September 2014

Pages: 11499 - 11516

[Image retargeting using nonparametric semantic segmentation]

Parvin Razzaghi & Shadrokh Samavi

OriginalPaper | Published: 20 September 2014

Pages: 11517 - 11536

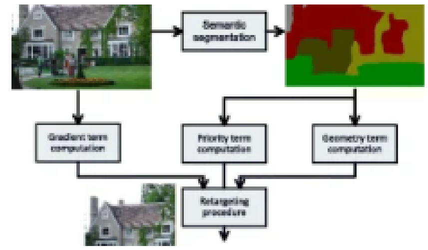

[Enhancing values through virtuality for intelligent artifacts that influence human attitude and behavior]

Mizuki Sakamoto, Tatsuo Nakajima & Todorka Alexandrova

OriginalPaper | Published: 03 September 2014

Pages: 11537 - 11568

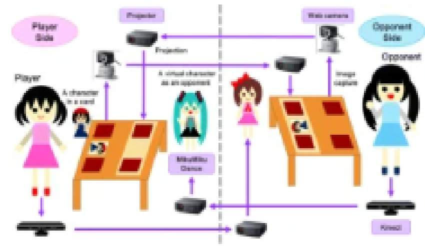

[Approximating adaptive distance measures using scalable feature signatures]

Jakub Lokoč

OriginalPaper | Published: 20 September 2014

Pages: 11569 - 11594

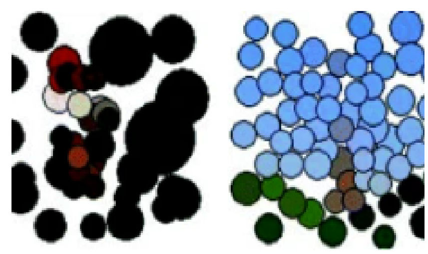

[Comparative assessment of efficiency for content based image retrieval systems using different wavelet features and pre-classifier]

Manish Chowdhury & Malay Kumar Kundu

OriginalPaper | Published: 21 September 2014

Pages: 11595 - 11630

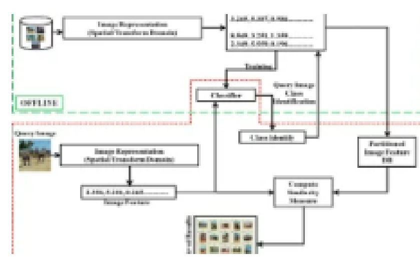

[K-motion: visualizing election information for live television broadcasts]

Kisun Yang & Taejung Park

OriginalPaper | Published: 16 September 2014

Pages: 11631 - 11651

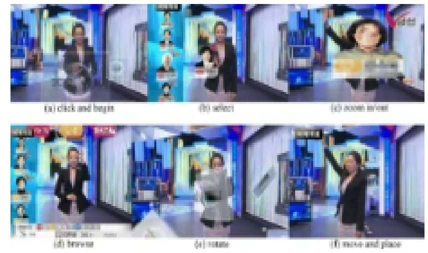

[Image hub explorer: evaluating representations and metrics for content-based image retrieval and object recognition]

Nenad Tomašev & Dunja Mladenić

OriginalPaper | Published: 10 September 2014

Pages: 11653 - 11682

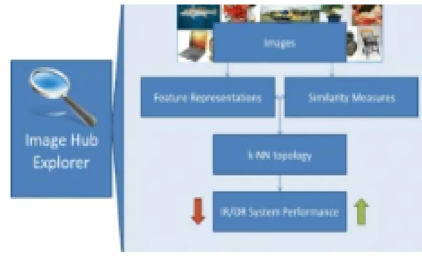

[Orientation range of transposition for vertical correlation suppression of 2DPalmPhasor Code]

Lu Leng, Andrew Beng Jin Teoh ... Muhammad Khurram Khan

OriginalPaper | Published: 09 September 2014

Pages: 11683 - 11701

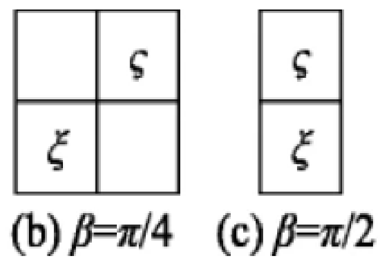

[An edge-preserving adaptive image denoising]

Xiang-Yang Wang, Yang-Cheng Liu ... Hong-Ying Yang

OriginalPaper | Published: 06 September 2014

Pages: 11703 - 11720

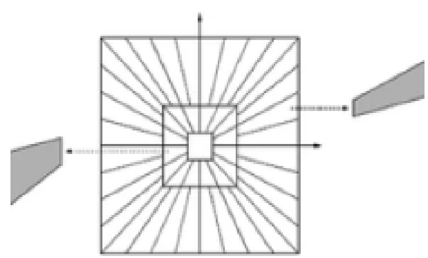

Blind watermarking scheme for polylines in vector geo-spatial data

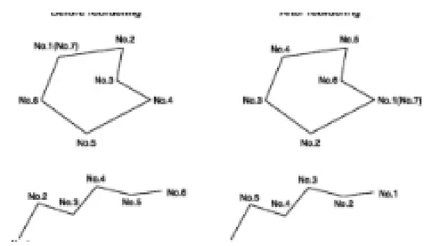

Zhiyong Peng, Mingliang Yue ... Yuwei Peng

OriginalPaper | Published: 13 September 2014

Pages: 11721 - 11739

Land cover classification using geo-referenced photos

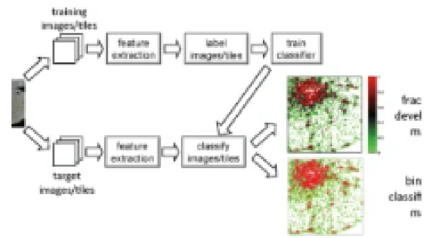

Daniel Leung & Shawn Newsam

OriginalPaper | Published: 19 September 2014

Pages: 11741 - 11761

A triple-layer steganography scheme for low bit-rate speech streams

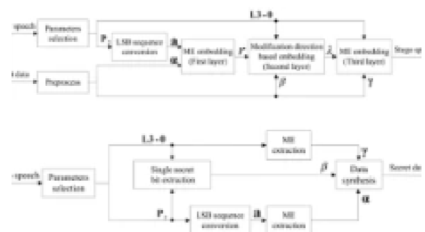

Shufan Yan, Guangming Tang ... Liuqing Shen

OriginalPaper | Published: 18 September 2014

Pages: 11763 - 11782

An overview of partial 3D object retrieval methodologies

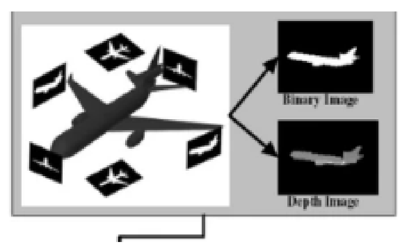

Michalis A. Savelonas, Ioannis Pratikakis & Konstantinos Sfikas

OriginalPaper | Published: 28 September 2014

Pages: 11783 - 11808

[CUDA-accelerated fast Sauvola's method on Kepler architecture](#)

Xin Chen, Yuefang Gao & Zhonghong Huang

OriginalPaper | Published: 23 September 2014

Pages: 11809 - 11820

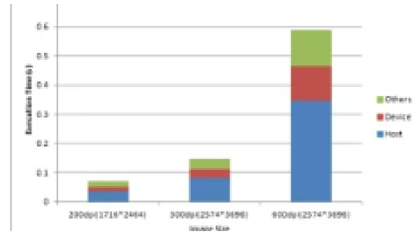

[A fast motion estimation algorithm based on adaptive pattern and search priority](#)

Jun Luo, Xiaohua Yang & Liheng Liu

OriginalPaper | Published: 25 September 2014

Pages: 11821 - 11836

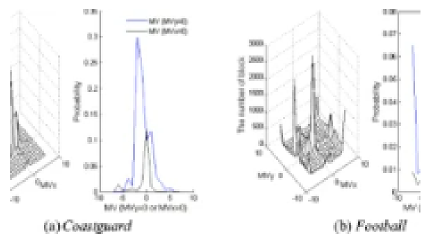

[Automatic pan-and-scan algorithm for heterogeneous displays](#)

Paween Khoenkaw & Punpiti Piamsa-nga

OriginalPaper | Published: 14 October 2014

Pages: 11837 - 11865

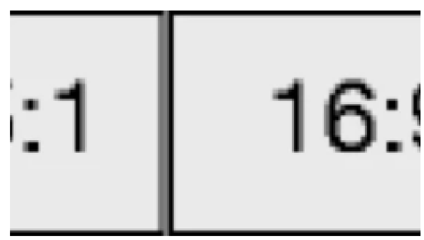

[Comments on "a robust logo watermarking technique in divisive normalization transform domain"](#)

Musrrat Ali & Chang Wook Ahn

OriginalPaper | Published: 17 December 2014 | Pages: 11867 - 11869

Multimed Tools Appl (2015) 74:11139–11161
DOI 10.1007/s11042-014-2222-9

Tree group based Wavelet Watermarking using Energy Modulation and Consistency Check (WW-EMCC) for digital images

Min-Jen Tsai · Jin-Sheng Yin · Imam Yuadi

Received: 14 November 2013 / Revised: 26 May 2014 / Accepted: 30 July 2014 /
Published online: 19 August 12014

Abstract Wavelet tree based watermarking algorithms are generally using the energy difference among grouped wavelet coefficients for invisible watermark embedding and extraction. According to cryptanalysis of wavelet tree quantization (WTQ) scheme, the robustness of watermarking is weak if the wavelet tree group coefficients are only unilaterally modulated. Therefore, bilaterally modulated techniques like modified wavelet tree quantization (MWTQ) and wavelet tree group modulation (WTGM) improve the security since the attackers can not decipher how tree coefficients are modulated. However, MWTQ needs the wavelet tree group information as the extra information which results the method is not purely blind for watermark extraction. For that matter, a novel wavelet tree group based watermarking using energy modulation and consistency check (WW-EMCC) is proposed in this study which not only resists the cryptanalysis attacks but also provides the dual function of choices for blind (WW-$EMCC_B$) and non-blind (WW-$EMCC_N$) watermark embedding. The essence of WW-EMCC design is to embed the watermark in the tree group coefficients as well as the relationship between the tree groups. Such approach extends the bilateral modulation into higher dimension of modulation and increase the robustness of security. In addition, WW-EMCC can even be modified as a captioning watermarking with lossless image quality which integrates watermarking and cryptography for copyright protection. This study has performed intensive comparison for the proposed scheme with WTQ, MWTQ and WTGM under various geometric and nongeometric attacks. The experimental results demonstrate that the proposed technique yields better performance with higher degree of robustness.

Keywords Watermarking · Wavelet tree quantization · Wavelet Transform

1 Introduction

As digital images are widely available online or elsewhere, and because they are easy to be modified, necessary works are required to protect the copyright and the verification of the

M.-J. Tsai (✉) · J.-S. Yin · I. Yuadi
Institute of Information Management, National Chiao Tung University, 1001 Ta-Hsueh Road, Hsin-Chu, 300, Taiwan, Republic of China
e-mail: mjtsai@cc.nctu.edu.tw

embedded genuine information. Conventional cryptographic systems permit only valid principals (key holders) access to encrypted data. Once such digital data are decrypted, there is no way to track their reproductions or retransmissions. Over the last decade, digital watermarking [8] has been presented to complement cryptographic protection mechanisms and received significant attraction [9] due to the popularity of the Internet and demands for the ownership protection.

Among different categories of researches for digital watermarking, robust invisible image watermarking embeds the secret information into digital images without scarifying the image fidelity and the watermarked images are visibly identical to the original cover images. Such approach provides a wider application empirically since the technique is very crucial to counteract the various attacks of unauthorized modification. Therefore, the robust invisible watermarking plays an important role for effective copyright protection and ownership verification since robust watermarks could be resilient to many image processing operations.

Image watermarking schemes can be classified into two categories depending on the domain of watermark insertion and retrieval, i.e., the luminance intensity in the spatial domain [5, 9] and the transform coefficient magnitude in the frequency domain. [2, 10, 11, 21, 22, 24, 29, 30, 33]. Spatial domain watermarking embeds information by directly modifying the value of image pixels, e.g., replacing the least significant bit (LSB) of image pixels with a binary pseudorandom noise (PN) sequence as watermark information. However, spatial domain watermarking is prone to be removed or modified and generally less robust than frequency domain watermarking.

The basic idea of frequency domain watermarking is to modify frequency coefficients after a proper transform, such as the DCT (Discrete Cosine Transform), DFT (Discrete Fourier Transform), DWT (Discrete Wavelet Transform). Because frequency-domain watermarking schemes tend to achieve both perceptual transparency and robustness requirements, various related algorithms have been developed [2, 8, 10, 11, 21, 22, 24, 29, 30, 33].

An et al. [4] developed a pragmatic framework for RRW (robust reversible watermarking) via clustering and EPWM (enhanced pixel-wise masking). On the other hand, histogram-based lossless data embedding [14] is secure for copyright protection if side information transmission is available. Feature-based image watermarking scheme [15] which aims to survive various geometric distortion also have attracted attention for researchers. Ritchey and Rego [25] presented a stego-system which generates stego-objects using context sensitive tiling. Huang and Fang [16] integrate the EXIF metadata of images and error-control codes with watermarking for copyright protection of images. Chan at al. [6] present a user-friendly system based on the use of JPEG- LS median edge predictor to determine the prime number for each block.

Most frequency-domain watermarking schemes are based on the additive spread-spectrum method, which is inspired by the spread-spectrum modulation technique in digital communication systems. The spread-spectrum watermarking scheme can resist more serious content distortion. Cox et al. [8] proposed a global DCT-based spread spectrum approach to hide watermarks. The frequency domain of the image or sound is viewed as a communication channel, and correspondingly, the watermark is viewed as a signal that is transmitted through it. The watermark is spread over many frequency bins so that the energy in any one bin is very small and certainly undetectable.

Langelaar and Lagendijk [21] introduced the DEW (Differential Energy Watermarking) algorithm for JPEG/MPEG streams in the DCT domain. The DEW algorithm embeds label bits (the watermark) by selectively discarding high frequency DCT coefficients in certain image regions. Das, Maitra and Mitra had presented a successful cryptanalysis against the DEW scheme in [10] and proposed a more robust scheme.

On the other hand, Wang and Lin [33] introduced the technique of WTQ (Wavelet Tree Quantization) in the DWT domain. The wavelet coefficients are grouped into so-called super trees. The wavelet tree based watermarking algorithm embeds watermark bits by selectively quantizing the super trees (such action can be categorized as unilateral modulation). Even if the attacker has no knowledge of which two trees are used for embedding, he can still quantize those super trees that are not quantized earlier with respect to the estimated quantization indices. Das and Maitra had presented how this could be accomplished in [11] by using cryptanalysis approach to attack WTQ. Since the weakness of WTQ could not provide the security promise of watermarking, Das and Maitra [11] had proposed a modified WTQ (MWTQ) algorithm which essentially used the positive and negative modulation (bilateral modulation) [22] to embed the watermark instead of quantization to defy the cryptanalysis attack. In general, the MWTQ scheme is similar to the wavelet tree group modulation (WTGM) [29, 30] technique which not only adopts the sum-of-subsets strategy [21] to efficiently group the wavelet trees but also further uses the contrast sensitive function (CSF) [17] and noise visibility function (NVF) [32] of human visual system for the better visual quality of the watermarked image. Another study of wavelet watermarking called ABW-TMD from [2] applied the wavelet tree mutual difference where the total embedding error is minimized by investigating which tree pairs will be allowed to embed the watermark bit and the embedding position will be saved as a sequential value in a private key. Even this design shows superior results to resist various image processing attacks than WTQ, the existence of the private key containing the watermark embedding location indicates such watermarking technique can not be categorized as "blind" watermarking approach. In summery, MWTQ, WTGM and ABW-TME all need the storage of the wavelet tree grouping information to extract the watermark which makes the algorithms essentially not blind and hinders the general use practically.

Furthermore, it is possible to extend the bilateral modulation into higher dimensional modulation for watermark embedding in order to increase the robustness of security under cryptanalysis. Therefore, this study investigates how to embed the watermark in the tree group coefficients as well as the relationship between the tree groups. The remainder of this paper is organized as follows. In Section 2, the proposed WW-EMCC watermarking method is introduced and explained in details. The experimental results and discussion are given in Section 3. Conclusion is in Section 4.

2 The proposed watermarking algorithm: WW-EMCC

In this study, we propose the tree group based wavelet watermarking using energy modulation and consistency check (WW-EMCC). The proposed WW-EMCC contains dual mode: one mode is the blind watermarking where the tree group information will not be needed (called WW-EMCC$_B$) and the other one is the non-blind watermarking where the tree group information can be stored as the key (called WW-EMCC$_N$). For comparison purpose, both modes will be introduced and their performance will be illustrated in Sec. 3.

2.1 WW-EMCC$_B$ concept and procedures

The host image is first applied by 4 level DWT transform as shown in Fig. 1 and collocate coefficients in $C_{i,j}$, where $i=\{2, 3, 4\}$ and $j=\{1, 2, 3\}$, to form the groups in Fig. 1. A tree has 21 coefficients: 1 coefficient from level-4, 4 coefficients from level-3, and 16 coefficients from

Fig. 1 Image after four-level wavelet decomposition

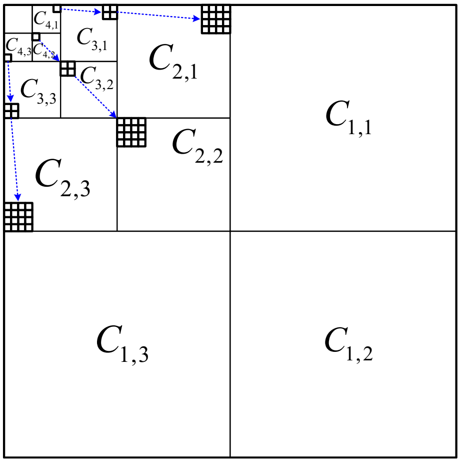

level-2. Let us define the energy g_r of a tree r as the sum of absolute value of all the 21 wavelet coefficients of that tree and their relationship is defined in Eq. (1).

$$g_r = \sum_{j=1}^{21} \left| x_j^r \right| \tag{1}$$

After building trees, the tree groups are randomly permuted by a permutation π prior to the construction of supertrees and theπis a secret information to the owner. Therefore the ordering of the trees is as $g_{\pi(1)}, g_{\pi(2)}, \ldots, g_{\pi(4n)}$ where $4n$ is the total number of available tree groups. Assume a supertree consists of l trees and energy β_k of supertree T_k is the sum of the constituent tree group energy, i.e.

$$\beta_k = \sum_{i=1}^{l} g_{\pi[(k-1)l+i]} \tag{2}$$

Assume there are two supertrees T_1, T_2, and their energies are β_1, β_2 respectively. If $\beta_1 \geq \beta_2$ before the attack, the energy relationship after attack could be $\beta_1 \geq \beta_2$ or $\beta_1 < \beta_2$. The larger difference between β_1 and β_2 is, the change of β_1 and β_2 relationship would be less possible. In order to embed the watermark effectively, modulation of T_1, T_2 is necessary. In addition, the relationship of T_1, T_2 can be used for verification. Therefore, another supertree pairs can be modified to enclose this checking data so WW-EMCC utilizes the positive and negative modulation analysis in [22] to embed the watermark not only in the tree group coefficients but also the relationship between tree groups. Under such consideration, four supertrees T_k, T_{k+1}, T_{k+2}, T_{k+3} will be randomly selected and their energies are β_k, β_{k+1}, β_{k+2}, β_{k+3} respectively. Those four supertrees are arranged into two pairs based on their energy difference. From the calculation of $\min\{|\beta_k - \beta_{k+1}|, |\beta_{k+2} - \beta_{k+3}|\}$, WW-EMCC calls the supertree pair with minimum difference value the MST (Modulated Supertrees), and the other supertree pair is called CST (Check Supertrees). As named above, the supertrees of MST will be used for modulation purpose and supertrees of the CST will be applied for checking the energy-modulated direction. The reason to modulate MST pair is to embed the watermark efficiently since the difference of MST pair is smaller than the one between CST pair. On the other hand, the checking information will be enclosed in CST pair because their difference is larger than MST pair.

Here we define the difference of MST pair as MSDV (modulated supertree difference value), and the difference of CST pair as CSDV (checking supertree difference value). MSDV and

CSDV are either positive or negative. The polarity of multiplication of MSDV and CSDV will be verified in order to embed the watermark bits since the watermark sequence is a binary PN (±1) sequence of watermark bits. While watermark=1, we want to make MSDV×CSDV>0 (i.e. $\beta_k > \beta_{k+1}$ and $\beta_{k+2} > \beta_{k+3}$ or $\beta_k < \beta_{k+1}$ and $\beta_{k+2} < \beta_{k+3}$). While watermark=−1, we want MSDV×CSDV≤0 (i.e. $\beta_k \geq \beta_{k+1}$ and $\beta_{k+2} \leq \beta_{k+3}$ or $\beta_k \leq \beta_{k+1}$ and $\beta_{k+2} \geq \beta_{k+3}$). If the modulation of MST is robust enough and the CSDV is also large enough, the energy relationship before and after attack among supertrees should be remained the same and we call this is the consistency check. This is the reason that we are using energy modulation and consistency check for watermarking. The detailed watermark embedding procedures of WW-EMCC $_B$ are following and the flow chart of watermark embedding procedures is shown in Fig. 2:

- WW-EMCC$_B$ watermark embedding algorithm:

1. Seed Generation. (Generate a seed by mapping a signature/text through a one-way deterministic function. Obtain a PN sequence ω of length N_w using the seed.)
2. Wavelet decomposition of the host image. (Compute wavelet coefficients of a host image by the pyramidal decomposition structure.)
3. Supertree construction. (Group the coefficients to form trees and every l trees will be used to construct a supertree in pseudorandom manner using the seed generated in step 1.)
4. For each watermark bit w_k (k=0 ; k<N_w – 1; k=k+4)

    a. Select the super trees T_k, T_{k+1}, T_{k+2}, T_{k+3} to embed watermark bit w_k.
    b. Compute the energy β_k, β_{k+1}, β_{k+2}, β_{k+3} of T_k, T_{k+1}, T_{k+2}, T_{k+3} respectively.
    c. Get MST$_k$ (Modulated Supertrees) tree pair from min{|β_k - β_{k+1}|,|β_{k+2} - β_{k+3}|} and the other supertree pair CST$_k$ (Check Supertrees).
    d. IF (w_k=1) then

        IF CSDV$_k$ > 0
            IF MSDV$_k$<= 0 , then continue.
            Else modulate the supertree pair of MST$_k$ to make MSDV$_k$<0 by the modulation format II.
            ELSE
            IF CSDV$_k$>0
            IF MSDV$_k$<= 0, then continue.
            Else modulate the supertree pair of MST$_k$ to make MSDV$_k$ <0 by the modulation format II.

    ELSE
        IF CSDV$_k$ > 0
            IF MSDV$_k$>0 , then continue.
            Else modulate the supertree pair of MST$_k$ to make MSDV$_k$>0 by the modulation format I.

5. Go to step 4 if k<N_w – 1.
6. Image reconstruction. (Pass the modified wavelet coefficients through the inverse DWT to obtain a watermarked image.)

Remarks:

1. **Modulation format I:**

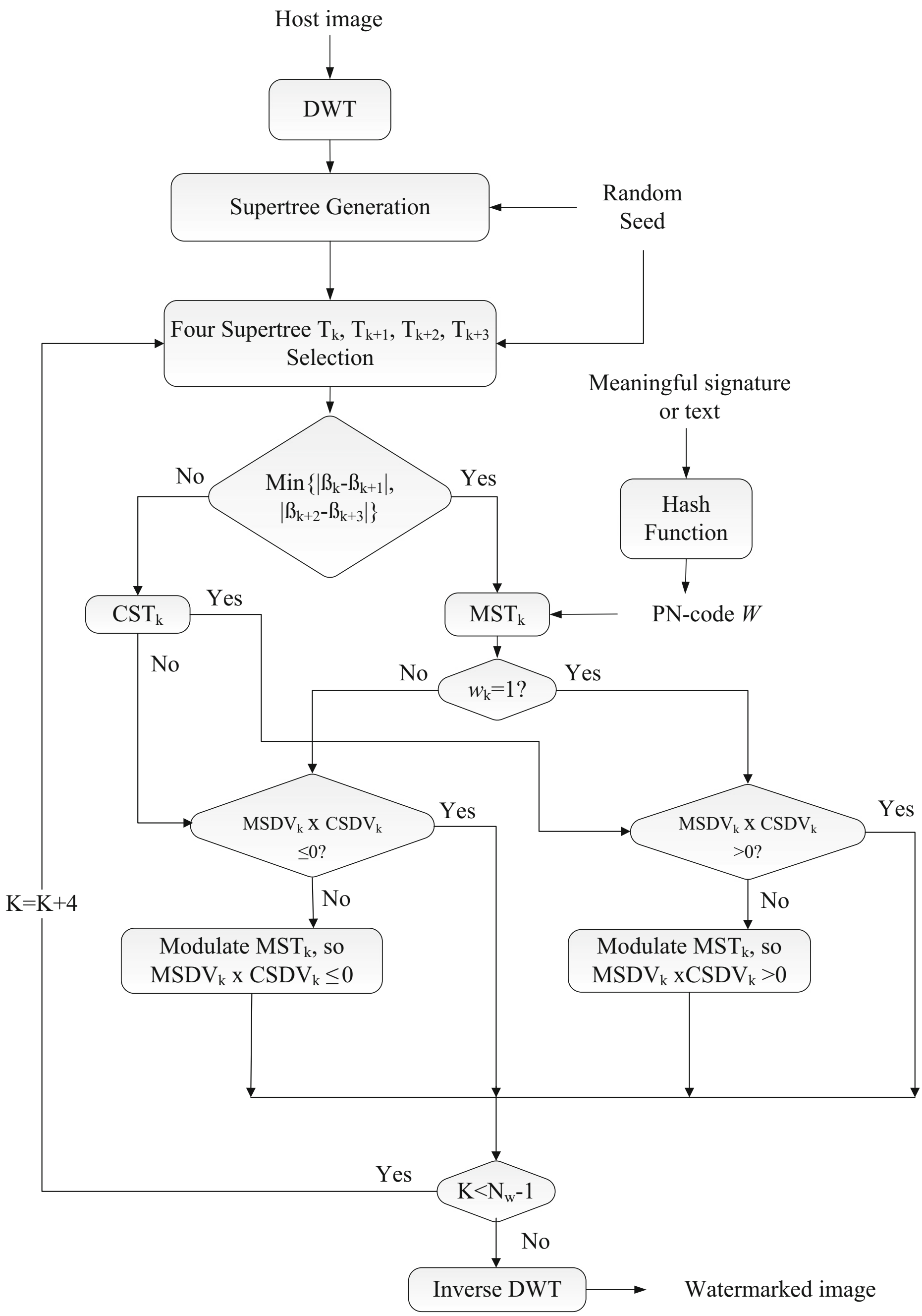

Fig. 2 Flow chart of watermark embedding for WW-EMCC$_B$

If two supertrees in MST pair are T_a and T_b, their sum of energy relationship is $\beta_b > \beta_a$. What we need to do is to make $\beta_b < \beta_a$. Therefore, we define $v = \sqrt{\beta_b/\beta_a} + \Delta$, Δ

is the control variable. For wavelet coefficient $x \in T_a$, $x=x\times v$ and for wavelet coefficient $x \in T_b$, $x=x/v$.

2. **Modulation format II:**

If two supertrees in MST pair are T_a and T_b, their sum of energy relationship is $\beta_b < \beta_a$. What we need to do is to make $\beta_b > \beta_a$. Therefore, we define $v = \sqrt{\beta_b/\beta_a} + \Delta$, Δ is the control variable. For wavelet coefficient $x \in T_a$, $x=x/v$ and for wavelet coefficient $x \in T_b$, $x=x\times v$.

For watermarking extraction, WW-EMCC$_B$ only needs the random seed to rebuild supertrees. After supertrees are reconstructed, the polarity of $(\beta_k - \beta_{k+1})\times(\beta_{k+2} - \beta_{k+3})$ value is examined to verify the watermark bit. If $(\beta'_k - \beta'_{k+1})\times(\beta'_{k+2} - \beta'_{k+3}) > 0$, the value of watermark bit=1. Otherwise, watermark bit=−1. To quantify the existence of the watermark after all watermark bits are extracted from the decoder (w'_k), the normalized correlation (NC) coefficient [33] will be examined in order to identify the existence of the watermark.

3. **Analysis of the probability of false positive [20]**:

A given watermark is detected if the correlation of the extracted watermark with the given watermark is above a pre-specified threshold. More precisely, the watermark detection condition is given by

$$\rho\left(\omega, \varpi\right) = \frac{\Sigma\omega(n)\varpi(n)}{\sqrt{\Sigma\omega^2(n)}\sqrt{\Sigma\varpi^2(n)}} \geq T \tag{3}$$

Where ω is the given watermark, ϖ is the extracted one, and T is a pre-specified threshold. The quantity $\rho\ (\omega,\varpi)$ is known as the correlation coefficient between the given and extracted watermarks.

Here we provide the analysis to estimates the probability of a false positive (i.e., false watermark detection) for the proposed technique. Here we define the probability of false watermark detection as

$$P_{fp} = P\{\rho(\omega,\varpi) \geq T | no\ mark\}, \tag{4}$$

Where $P\{A|B\}$ is the probability of event A given event B. We can rewrite $\rho\ (\omega,\varpi)$ as

$$\rho\left(\omega, \varpi\right) = \frac{\Sigma\omega(n)\varpi(n)}{\sqrt{\Sigma\omega^2(n)}\sqrt{\Sigma\varpi^2(n)}} = \frac{\Sigma\omega(n)\varpi(n)}{N_w} \tag{5}$$

Since $\omega(n)$ and $\varpi(n)$ are either one or negative one, and subsequently $\omega^2(n) = \varpi^2(n) = 1$ and index n ranges from 1 to N_w. Let p_E be the probability of bit error during extraction. A bit error occurs when $\varpi(n) \neq \omega(n)$ or more specifically, when $\varpi(n) = -\omega(n)$ (since $\omega(n), \varpi(n) \in \{-1,1\}$). If we let $\kappa(n)=\omega(n)\varpi(n)$, then $\kappa(n)=-1$ indicates a bit error and $\kappa(n)=1$ indicates no error. We may rewrite the expression for ρ and P_{fp} in terms of $\kappa(n)$ as

$$\rho\left(\omega, \varpi\right) = \frac{\Sigma\omega(n)\varpi(n)}{N_w} = \frac{\Sigma\kappa(n)}{N_w} \tag{6}$$

and

$$P_{fp} = P\left\{\sum\kappa(n) \geq N_w T \middle| \text{no mark}\right\} \tag{7}$$

respectively. Since $\kappa(n) \in \{-1, 1\}$, it can be shown that $\sum\kappa(n)$ must take on discrete values on the set $\{-N_w, -N_w+2, -N_w+4, \ldots, N_w-4, N_w-2, -N_w\}$, or $\sum\kappa(n) = -N_w + 2m$, where $m = 0, 1, \ldots, N_w$. Thus, we find that

$$P_{fp} = P\left\{\sum\kappa(n) \geq N_w T \middle| \text{no mark}\right\} = \sum_{m=\lceil N_w(T+1)/2 \rceil}^{N_w} P\left\{\Sigma\kappa(n) = -N_w + 2m \middle| \text{no mark}\right\} \tag{8}$$

Where $P\{\Sigma\kappa(n) = -N_w + 2m \mid \text{no mark}\}$ is the probability that the series $\{\kappa(n)\}$ contains m ones and $N_w - m$ negative ones. The lower bound is $\sum\kappa(n) = N_w T$ which can derive the probability of lower bound based on the summation for $m = \lceil N_w(T+1)/2 \rceil$. Therefore,

$$P_{fp} = P\left\{\sum\kappa(n) = -N_w + 2m \middle| \text{no mark}\right\} = \binom{N_w}{m} p_E^{N_w - m}(1 - p_E)^m \tag{9}$$

Where p_E is the probability that $\kappa(n) = -1$ and $\binom{N_w}{m} = \frac{N_w!}{m!(N_w - m)!}$. Since we are given that no watermark is embedded, we can assume that the extracted mark ϖ consist of a series of random independent equally probable value from the set $\{-1, 1\}$. Thus, $pE = 0.5$. Substituting into Eqs. (8) and (9),

$$P_{fp} = \sum_{m=\lceil N_w(T+1)/1 \rceil}^{N_w} \binom{N_w}{m} 0.5^{N_w} \tag{10}$$

Given a desired probability of false alarm, we can set the threshold T using Eq. (10). As the length of the watermark increases, the probability of false detection decreases for a fixed threshold. The choice of threshold should be a function of N_w and must be application-dependent.

The normalized correlation coefficient value is within −1 and 1. The existence decision is "yes" if $\rho\,(\omega, \varpi)$ and "no" if $\rho\,(\omega, \varpi) < T$. The threshold T is chosen based on the probability of false positive error P_{fP} from (10). Given the reasonable assumption, $P_E = 0.5$ and $N_w = 512$ as the watermark length, T is chosen to be 0.23 while P_{fp} will be as low as 1.03×10^{-7}. That means the appropriate T will be selected to meet the requirement given a false positive probability. If watermark length is decreased from 512 to 64, the threshold T should be increased in order to maintain a low false positive probability P_{fP}. Under such circumstance, T will be selected as 0.5 to achieve P_{fp} as low as 3.86×10^{-5}. Those values will be applied in Sec. 3 for experimental demonstration.

4. **Watermark capacity analysis:**

For the proposed WW-EMCC watermarking algorithm, a tree has 21 coefficients after 4 level wavelet pyramidal decomposition which forms the super tree T and the algorithm randomly selects 4 super trees T_k, T_{k+1}, T_{k+2}, T_{k+3} to embed each watermark bit w_k. For the 512×512 host image, there are total of $3\times32^2=3072$ trees and 3072/4=768 bits can be embedded. In WTQ, two tree groups to from a super trees and each watermark bit is embedded using two super trees. For the 512×512 host image, the maximum number of watermark bits that can be embedded is thus 1536/2=768 [33]. The difference between WTQ, MWTQ and WTGM is that the super tree selection in WTQ is random but the selection in MWTQ and WTGM is based on the sorting of the energy summation through the trees. Therefore, MWTQ and WTGM need the record of the super tree ordering [11, 30] which also has the same maximum number of embedding watermark bits. In summary, the most possible watermark capacity is 768 for WW-EMCC which is equivalent to the maximum number of embedding watermark bits for WTQ [33], MWTQ [11] and WTGM [30] algorithms. Thus, WW-EMCC, WTQ, MWTQ and WTGM algorithms all have the same maximum watermark capacity through the design.

The detailed watermark extraction procedures of WW-EMCC $_B$ are following and the flow chart of watermark extraction is shown in Fig. 3:

- WW-EMCC$_B$ watermark extraction algorithm:

1. Seed Generation. (Generate a seed by mapping a signature/text through a one-way deterministic function. Obtain a PN sequence W of length N_w using the seed.).
2. Tree construction from the watermarked image. (Compute wavelet coefficients of a received host image by the pyramidal decomposition structure. Group the coefficients to form trees and every l trees will be used to constructed a supertree in pseudorandom manner using the seed generated in step 1.)
3. For each watermark bit w'_k (k=0 ; $k<N_w-1$; $k=k+4$)

   a. compute the energy β'_k, β'_{k+1}, β'_{k+2}, β'_{k+3} of T'_k, T'_{k+1}, T'_{k+2}, T'_{k+3} espectively.
   b. If $(\beta'_k-\beta'_{k+1})\times(\beta'_{k+2}-\beta'_{k+3})>0$, $w'_k=1$

   Else $w'_k=-1$

4. Go to step 3 if $k<N_w-1$.
5. Using Eq. 3 to compute the normalized correlation coefficient ρ.
6. If ρ is above the threshold T, the watermark W exists; otherwise, it does not exist.

2.2 WW-EMCC$_N$ concept and procedures

Since WW-EMCC$_N$ allows the existence of the supertree group information during watermark extraction as a private key, it provides the freedom to select the supertrees during watermark embedding. Thus the energy of the supertrees can be calculated in advance and the supertree can be numbered in a descending order as T_0, T_1, T_2, … and $\beta_0\geq\beta_1\geq\beta_2\geq\beta_3$ …respectively. The information about the ordered supertrees is stored in a location list λ. λ_0 contains the tree information of the largest supertree, λ_1 contains the tree information of the next largest supertree, … etc. During the watermark embedding procedure, a key list Φ will store the tree information from location list λ and Φ_0 will contain the first suptertree group information, Φ_1 will contain the next supertree group information, …etc.

In order to embed each watermark bit, WW-EMCC$_N$ random select the super trees from the location list λ sequentially. Suppose the selected supertees are T_a, T_b, T_c, T_d and $a<b<c<d$.

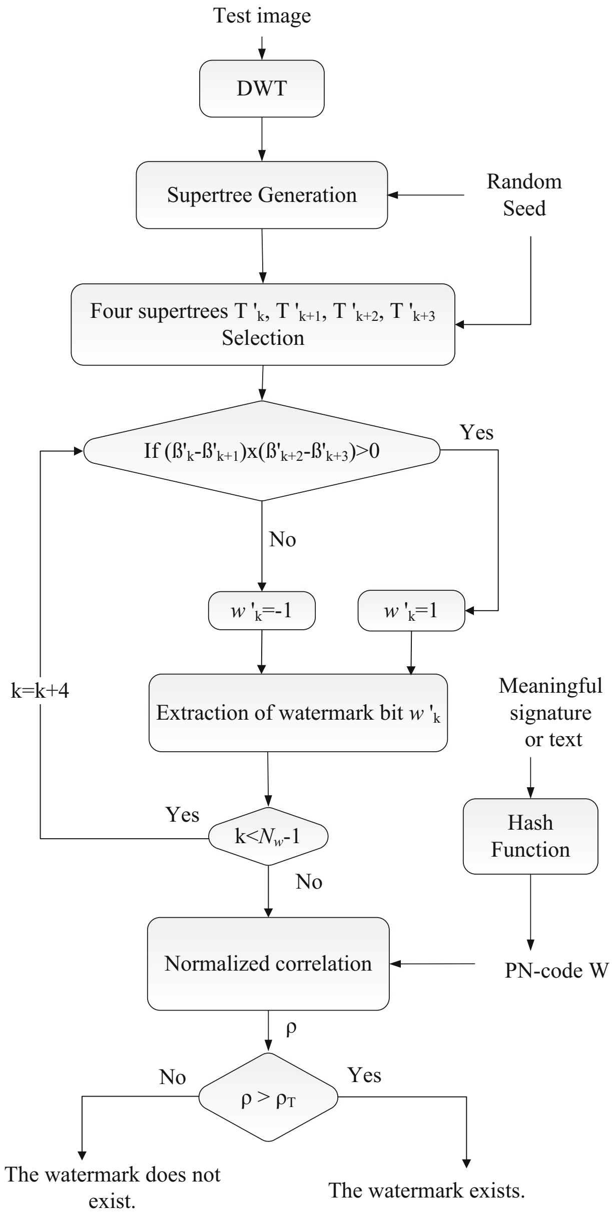

Fig. 3 Flow chart of watermark extraction for WW-EMCC$_B$

Therefore, the tree information about T_a, T_b, T_c, T_d will be recorded to a key list Φ from location list λ during the watermark embedding procedure and the group information of T_a, T_b, T_c, T_d will be removed from the location list λ. Since the energy relationship of supertree pair will disclose what the watermark bit is, some supertree order will be modified based on the polarity of the watermark bit. Based on such fact, the energy modulation in

WW-EMCC$_B$ is not needed at all for WW-EMCC$_N$ procedures. The cover image can even remain the same without any change which we call this is the lossless watermarking for WW-EMCC$_N$.

After all watermark bits are embedded, the key list Φ will store the rest of tree information from the location list λ if there are still supertees left without watermark embedding. Accordingly, the key list Φ will later be used as a private key during the watermark extraction since it enclose all the supertree grouping information. The detailed watermark embedding procedures of WW-EMCC$_N$ are as following:

- WW-EMCC$_N$ watermark embedding algorithm:

1. Seed generation. (Generate a seed by mapping a signature/text through a one-way deterministic function. Obtain a PN sequence W of length N_w using the seed.)
2. Wavelet decomposition of the host image. (Compute wavelet coefficients of a host image by the pyramidal decomposition structure. Group the coefficients to form trees and every l trees will be used to construct a supertree in pseudorandom manner using the seed generated in step 1.)
3. Supertree ordering. (Order the supertrees in a descending order based on the energy summation of the supertree wavelet coefficients. The information about the ordered supertrees is stored in a location list λ.)
4. For each watermark bit w_k (k=0 ; $k<N_w-1$; $k=k+4$)
   a. Randomly select 4 super trees from the location list λ sequentially. Assume the selected supertees are T_a, T_b, T_c, T_d and $a<b<c<d$.
   b. IF (w_k=1)

      IF Rand() % 2=0 then
      Store the group information of T_a from location list of λ to Φ_k.
      Store the group information of T_b from location list of λ to Φ_{k+2}.
      Store the group information of T_c from location list of λ to Φ_{k+1}.
      Store the group information of T_d from location list of λ to Φ_{k+3}.
      ELSE
      Store the group information of T_a from location list of λ to Φ_{k+2}.
      Store the group information of T_b from location list of λ to Φ_k.
      Store the group information of T_c from location list of λ to Φ_{k+3}.
      Store the group information of T_d from location list of λ to Φ_{k+1}.
      ELSE
      IF Rand() % 2=0 then
      Store the group information of T_a from location list of λ to Φ_k.
      Store the group information of T_b from location list of λ to Φ_{k+2}.
      Store the group information of T_c from location list of λ to Φ_{k+3}.
      Store the group information of T_d from location list of λ to Φ_{k+1}.
      ELSE
      Store the group information of T_a from location list of λ to Φ_{k+2}.
      Store the group information of T_b from location list of λ to Φ_k.
      Store the group information of T_c from location list of λ to Φ_{k+1}.
      Store the group information of T_d from location list of λ to Φ_{k+3}.

   c. Remove the group information of T_a, T_b, T_c, T_d from the location list λ.
5. Go to step 4 if $k<N_w-1$.

6. Image Reconstruction. (Pass the modified wavelet coefficients through the inverse DWT to obtain a watermarked image.)

Remarks:

While location list λ is not empty, the key list Φ will store the rest of tree information from the location list λ since there are still supertees left without watermark embedding. Use the key list Φ during the watermark extraction as a private key. Pass the modified wavelet coefficients through the inverse DWT to obtain a watermarked image. Through the steps of WW-EMCC$_N$, the watermarked image is actually identical to the original cover image since there is no coefficient change procedure. Some researchers may criticize whether such a design is the watermarking algorithm or not if the cover image is not modified. To satisfy such the requirement, we can easily adjust WW-EMCC$_B$ into a lossy version of WW-EMCC$_N$. The procedures are following:

- Lossy version of WW-EMCC$_N$ algorithm:

1. Seed Generation. (Generate a seed by mapping a signature/text through a one-way deterministic function. Obtain a PN sequence ω of length N_w using the seed.)
2. Wavelet decomposition of the host image. (Compute wavelet coefficients of a host image by the pyramidal decomposition structure.)
3. Supertree ordering. (Order the supertrees in a descending order based on the energy summation of the supertree wavelet coefficients. The information about the ordered supertrees is stored in a location list λ.)
4. For each watermark bit w_k (k=0 ; k<N_w – 1; k=k+4)

   a. Sequentially select 4 super trees T_k, T_{k+1}, T_{k+2}, T_{k+3} to embed watermark bit w_k.

   b. c. d. are the same steps as 4.b, 4.c, 4.d of **WW-EMCC$_B$**.

5. same as step 5–6 of **WW-EMCC$_B$**

Therefore, the lossy version of WW-EMCC$_N$ will go through the modulation procedures as WW-EMCC$_B$. The location list λ will be the private key during the watermark extraction. However, the benefit of the supertree sorting will make the minimum change during the modulation for each supertree pair and also improve the robustness for the watermarked images under attacks.

In addition, the lossless and lossy version of WW-EMCC$_N$ use the same watermark extraction algorithm where the only difference is the private key. The private key for lossless version of WW-EMCC$_N$ is the key list Φ and lossy version of WW-EMCC$_N$ use the location list λ. The detailed watermark extraction procedures of WW-EMCC $_N$ are as follows.

- WW-EMCC$_N$ **watermark extraction algorithm:**

1. Seed generation. (Generate a seed by mapping a signature/text through a one-way deterministic function. Obtain a PN sequence W of length N_w using the seed.)
2. Wavelet coefficient reconstruction. (Compute the wavelet coefficients of a received host image by the pyramidal decomposition structure.)
3. Tree grouping. (Group the coefficients to form trees using the private key during the watermark embedding.)

4. For each watermark bit w_k' (k=0 ; $k<N_w-1$; k=k+4)

   a. Select the supertrees T'$_k$, T'$_{k+1}$, T'$_{k+2}$, T'$_{k+3}$ and compute the energy β'_k, β'_{k+1}, β'_{k+2}, β'_{k+3} respectively using the private key.
   b. If $(\beta'_k-\beta'_{k+1})\times(\beta'_{k+2}-\beta'_{k+3})>0$, $w_k'=1$

   Else $w_k'=-1$

5. Go to step 3 if $k<N_w-1$.
6. Using Eq. 3 to compute the normalized correlation coefficient ρ.
7. If ρ is above the threshold T, the watermark W exists; otherwise, it does not exist.

3 Experiments and discussion

WW-EMCC can provide either a blind or a non-blind version of watermarking technique. To be honest, it is unfair to compare the robustness under attacks between the blind watermarking technique and the non-blind watermarking method. The reason is that the non-blind watermarking method has the advantage of the side information to preserve more information and can provide better robustness over the blind watermarking technique. In essence, MWTQ [11] and WTGM [30] rely on the tree group ordering information for watermark extraction so both of them are non-blind watermarking techniques. Since the proposed WW-EMCC algorithm is a new approach for both the blind and the non-blind watermarking methods, this research does extensive studies to compare MWTQ, WTGM with WW-EMCC$_N$ for the non-blind watermarking method, and compare WTQ with WW-EMCC$_B$ for the blind watermarking method.

To evaluate the performance of the proposed method, we have investigated the results of the proposed techniques for a wide range of image databases including [13, 19, 31]. The performance under proposed WW-EMCC achieves very good robustness against attacks. The authors really like to demonstrate the testing results using the images within those databases. However, it would be very controversial by the selection of the particular images which may be criticized for favoring the proposed WW-EMCC algorithm. Under such circumstance, the authors have no choice but to provide the testing results in details by using the well known images like Lena, Goldhill and Peppers from [31]. The selected images have different statistics. Lena combines uniform areas with texture and Goldhill contains mainly texture with different structure. Thus, Peppers have very large uniform areas, texture and rather moderate contrast within the object. All of the three test images are very often used in the literatures which provide benchmark testing statistics for the fair comparison. The 512×512 Lena, Goldhill and Peppers images with 8 bits/pixel resolution are illustrated in Fig. 4. for watermarking. In order to make the fair comparison, all the watermarked images will be set at the same PSNR values while the watermark length is different. Therefore, the PSNR values of Lena, Goldhill and Peppers are 38.2, 38.7 and 39.8 dB respectively for watermark length of 512 from [33] and 40.73, 41.10 and 40.46 dB respectively for watermark length of 64 from [11]. For example, the Δ setting of WW-EMCC$_B$ and lossy version WW-EMCC$_N$ for Lena, Goldhill and Peppers are tabulated in Table 1 for 512 bit watermark length. Table 1 tabulates all the delta values for WW-EMCC which explain how to get the same image quality for the fair comparison with WTQ, MWTQ and WTGM algorithms. Through the watermark extraction description in Sec. 2, there is no need for delta values during the extraction steps for either

(a) (b) (c)

Fig. 4 Classical graylevel test images: (a) Lena, (b) Goldhill and (c)Peppers

WW-EMCC$_B$ or **WW-EMCC$_N$** algorithms. Thus, the delta values are not preserved for watermark extraction which is the simplicity of the algorithm and applicable for practical usage. The detection threshold T of NC is chosen to be 0.23 as same as in [11, 30, 33] for 512 bit watermarks. However, [11] did not perform the NC analysis and T of NC should be 0.5 for 64 bit watermarks. The reason is explained in Sec. 2's remarks.

While the data in the tables with dark background means the NC values are below the threshold and the watermarks cannot be detected through the watermark detection procedures. All the results from common image processing attacks, geometric attacks and security measure will be tabulated for illustration purpose. Due to many experimental comparisons are performed in this study with limited space, we will illustrate the data as much as possible for demonstration purpose. Several symbols are used in The TABLEs where M represents MWTQ method, G represents WTGM method, Q represents WTQ method, B represents WW-EMCC$_B$ method and N represents WW-EMCC$_N$ method respectively.

3.1 Common image processing attacks

3.1.1 JPEG compression attacks

In this experiment, we perform JPEG compression with different quality factors (QF) on the watermarked images. The extracted results and NC values are depicted in Table 2. From these results, WW-EMCC$_B$ and WW-EMCC$_N$ have almost the same performance as MWTQ and WTGM while the watermark length is 64 bits. For watermark length is 512 bits, WW-EMCC$_N$ is comparable with MWTQ and WTGM, and WW-EMCC$_B$ outperforms WTQ in most of the settings. From Table 2, the extracted watermarks are with relatively high-NC values and the embedded watermark can be still detected even QF is equal to 30.

Table 1 Δ Setting of WW-EMCC for Lena, Goldhill and Pepper images with 512 bit watermark length

	Lena	Goldhill	Peppers
PSNR	38.2dB	38.7dB	39.8dB
WW-EMCC$_B$	Δ =0.35	Δ =0.45	Δ =0.20
WW-EMCC$_N$	Δ =0.15	Δ =0.15	Δ =0.13

Table 2 Correlation coefficient ρ upon attacks of JPEG compression with quality factor of 90, 70, 50, 40, 30 with different watermark length (a) Lena (b) Goldhill (c) Peppers

	64 bits			512 bits				
QF	MWTQ	WW-EMCC		MWTQ	WTGM	WTQ	WW-EMCC	
		Blind	Non-Blind				Blind	Non-Blind
(a)								
90	1.00	1.00	1.00	1.00	1.00	1.00	0.98	1.00
70	1.00	1.00	1.00	1.00	1.00	0.57	0.85	1.00
50	1.00	1.00	1.00	0.99	0.98	0.26	0.67	1.00
40	1.00	1.00	1.00	0.98	0.96	0.23	0.60	1.00
30	0.96	1.00	1.00	0.97	0.95	0.15	0.52	1.00
(b)								
90	1.00	1.00	1.00	1.00	1.00	1.00	0.98	1.00
70	1.00	1.00	1.00	1.00	1.00	0.93	0.92	1.00
50	1.00	1.00	1.00	0.99	0.99	0.71	0.87	1.00
40	1.00	1.00	1.00	0.99	0.98	0.52	0.83	1.00
30	0.93	1.00	1.00	0.99	0.95	0.23	0.75	1.00
(c)								
90	1.00	1.00	1.00	1.00	1.00	1.00	0.98	1.00
70	1.00	1.00	1.00	1.00	0.99	0.97	0.85	1.00
50	1.00	1.00	1.00	0.98	0.94	0.70	0.68	1.00
40	0.96	0.93	1.00	0.95	0.90	0.54	0.62	1.00
30	0.93	0.93	1.00	0.92	0.83	0.34	0.47	1.00

3.1.2 JPEG 2000 compression attacks

For JPEG 2000 compression, the software from [18] is applied and the experimental results of 64 bit watermark length are tabulated in Table 3. The settings are at 100:1, 100:2, 100:5, 100:7 and 100:9 compression ratios for Lena, Goldhill and Peppers images respectively. From Table 3, they are all with relatively high NC values even at the compression ratio of 100:1 for WW-EMCC$_B$. Apparently, the results of WW-EMCC$_B$ are comparable to those of MWTQ under JPEG 2000 compression attack.

Table 3 Correlation coefficient ρ upon attacks of JPEG 2000 compression with 64 bit watermark length (where M represents MWTQ method, B represents WW-EMCC$_B$ method and N represents WW-EMCC$_N$ method)

	Lena			Goldhill			Peppers		
Setting	M	B	N	M	B	N	M	B	N
0.01	0.59	0.59	0.84	0.50	0.53	0.65	0.40	0.65	0.84
0.02	0.81	0.84	0.96	0.78	0.71	0.93	0.79	0.84	0.96
0.05	1.00	1.00	1.00	1.00	0.93	1.00	0.98	0.96	1.00
0.07	1.00	1.00	1.00	1.00	0.90	1.00	1.00	0.96	1.00
0.09	1.00	1.00	1.00	1.00	0.93	1.00	1.00	0.96	1.00

3.1.3 SPIHT compression attacks

SPIHT (Set Partitioning in Hierarchical Trees) is an image compression algorithm that exploits the inherent similarities across subbands in a wavelet decomposition of an image. It implies uniform quantization and bit allocation applied after wavelet decomposition. Table 4 shows the extracted NC values between original watermark and extraction watermark for 512 bit watermark length. Since the results from MWTQ are not available from [11], the results of WTQ and WTGM are tabulated instead. From these results, we can see that results of WW-EMCC$_B$ and WW-EMCC$_N$ can tolerate the incidental distortions induced by high-quality SPIHT compression but WTQ can not.

3.1.4 Spatial-domain image processing attacks

Several spatial-domain image processing attacks include median filtering, Gaussian filtering, sharpening, contrast enhancement, and brightness enhancement are performed and the NC values are depicted in Table 5. For all cases, the watermark information therein can be successfully recognized and the proposed algorithms outperform the WTQ, MWTQ and WTGM schemes with relatively high-NC values.

3.2 Geometric attacks

3.2.1 Rotation attacks (Rotation and Scaling)

The attack is done by rotating the image by a small angle, scaling the rotated image, and cropping the scaled image to the original image size. StirMark [27] software is adopted here for this attack since it provides the described testing functions. In addition, the rotation operation (including scaling and cropping during the rotation) is performed by StirMark automatically. Accordingly, StirMark software is applied for WTQ, MWTQ, WTGM and WW-EMCC respectively. Since the parameters of scaling and cropping during the rotation are image dependent, only the final normalized correlation values are tabulated in Table 6 to avoid too many parameters in the tables.

Table 4 CORRELATion coefficient ρ upon attacks of SPIHT compression with 512 bit watermark length (where Q represents WTQ method, G represents WTGM method, B represents WW-EMCC$_B$ method and N represents WW-EMCC$_N$ method)

	Lena				Goldhill				Peppers			
Bit rate	Q	G	B	N	Q	G	B	N	Q	G	B	N
0.1	NA	NA	0.68	0.96	NA	NA	0.68	0.62	NA	NA	0.71	0.93
0.2	NA	NA	0.90	1.0	NA	NA	0.81	0.96	NA	NA	0.84	1.0
0.3	0.21	0.96	0.93	1.0	−0.06	0.95	0.87	1.0	0.36	0.64	0.96	1.0
0.4	0.41	0.98	1.0	1.0	0.02	0.97	0.90	1.0	0.66	0.98	1.0	1.0
0.5	0.85	0.99	0.96	1.0	0.23	0.99	0.90	1.0	0.65	0.98	1.0	1.0
0.6	0.83	0.99	1.0	1.0	0.27	1.0	0.96	1.0	0.71	1.0	1.0	1.0
0.7	0.85	1.0	1.0	1.0	0.35	1.0	0.93	1.0	0.85	1.0	1.0	1.0

Table 5 Correlation coefficient ρ upon attacks of spatial-domain image processing with 64bit and 512 bit watermark length (where M represents MWTQ method, G represents WTGM method, Q represents WTQ method, B represents WW-EMCC$_B$ method and N represents WW-EMCC$_N$ method)

	64 bits			512 bits				
	M	B	N	M	G	Q	B	N
(a)								
Median Filtering (2×2)	0.65	0.90	1.00	0.93	0.96	0.38	0.70	1.00
Median Filtering (3×3)	0.84	0.93	1.00	0.96	0.89	0.51	0.81	1.00
Median Filtering (4×4)	0.46	0.75	0.93	0.70	0.57	0.23	0.48	1.00
Gaussian Filtering	0.68	0.93	1.00	0.85	0.68	0.64	1.00	1.00
Sharpening	1.00	0.93	1.00	1.00	1.0	0.46	1.00	1.00
Contrast Enhancement (10%)	1.00	1.00	1.00	1.00	1.0	NA	1.00	1.00
Brightness Enhancement (10%)	1.00	1.00	1.00	1.00	1.0	NA	1.00	1.00
(b)								
Median Filtering (2×2)	1.00	0.87	1.00	0.95	0.93	0.35	0.76	1.00
Median Filtering (3×3)	0.87	0.96	1.00	0.98	0.85	0.56	0.89	1.00
Median Filtering (4×4)	0.75	0.87	0.90	0.81	0.65	0.24	0.66	1.00
Gaussian Filtering	0.59	1.0	0.87	0.94	0.80	0.56	1.00	1.00
Sharpening	0.62	1.00	1.00	1.00	1.0	0.39	1.00	1.00
Contrast Enhancement (10%)	1.00	1.00	1.00	1.00	1.0	NA	1.00	1.00
Brightness Enhancement (10%)	1.00	1.00	1.00	1.00	1.0	NA	1.00	1.00
(c)								
Median Filtering (2×2)	0.87	0.84	0.96	0.86	0.81	0.46	0.50	1.00
Median Filtering (3×3)	1.00	0.93	1.00	0.97	0.64	0.71	0.58	1.00
Median Filtering (4×4)	0.68	0.84	0.90	0.71	0.56	0.25	0.35	1.00
Gaussian Filtering	0.68	0.94	1.00	0.76	0.42	0.74	1.00	1.00
Sharpening	0.96	0.97	1.00	1.00	1.0	0.62	1.00	1.00
Contrast Enhancement (10%)	1.00	1.00	1.00	1.00	1.0	NA	1.00	1.00
Brightness Enhancement (10%)	1.00	1.00	1.00	1.00	1.0	NA	1.00	1.00

The attacked results are given in Table 6 and wavelet tree based schemes are generally not very robust against geometric attacks. From these results, we can see that WW-EMCC$_B$ and WW-EMCC$_N$ algorithms can resist the rotation up to ±1° for all three images while watermark length is 64 bits, MWTQ fails to resist the rotation attack for all three images. While watermark length is 512 bits, MWTQ can resist the rotation up to ±1° for all three images but WW-EMCC$_B$ can not. However, WW-EMCC$_N$ can resist the rotation up to ±3° for all three images which shows its robustness is superior to MWTQ and WTGM.

3.3 Security measurement

3.3.1 Multiple watermarking

The attacker may apply one or more watermarks using the same wavelet tree watermarking technique in an attempt to confuse the detector or to destroy the embedded watermark. Table 7 gives the results while the images are attacked through multiple watermarking. From the statistics, the proposed scheme can resist up to four watermark attacks but WTQ can only resist

Table 6 Correlation coefficient ρ and watermark existence upon attacks of rotation, followed by scaling and cropping to the original size with different watermark length. (a) Lena (b) Goldhill (c) Peppers

	64 bits			512 bits				
Rotation(。)	MWTQ	WW-EMCC		MWTQ	WTGM	WTQ	WW-EMCC	
		Blind	Non-Blind				Blind	Non-Blind
(a)								
−0.50	0.47	0.65	0.84	0.71	0.98	0.23	0.32	0.99
−0.75	0.37	0.65	0.65	0.52	0.95	0.24	0.16	0.98
−1.00	0.21	0.65	0.56	0.37	0.89	0.16	0.15	0.96
−3.00	0.0	0.15	0.28	0.14	0.23	NA	0.0	0.58
0.50	0.47	0.68	0.90	0.64	0.96	0.29	0.31	0.99
0.75	0.37	0.59	0.75	0.42	0.90	0.26	0.21	0.96
1.00	0.25	0.46	0.62	0.33	0.88	0.24	0.17	0.93
3.00	0.0	0.28	0.34	0.05	0.33	NA	0.0	0.52
(b)								
−0.50	0.47	0.71	0.62	0.71	0.95	0.27	0.50	0.95
−0.75	0.37	0.71	0.50	0.56	0.89	0.25	0.53	0.93
−1.00	0.25	0.46	0.40	0.44	0.82	0.14	0.34	0.89
−3.00	0.0	0.12	0.28	0.00	0.24	NA	0.0	0.46
0.50	0.40	0.65	0.59	0.68	0.95	0.24	0.50	0.98
0.75	0.25	0.50	0.59	0.56	0.91	0.21	0.50	0.93
1.00	0.12	0.37	0.46	0.50	0.88	0.15	0.28	0.89
3.00	0.0	0.28	0.21	0.09	0.34	NA	0.0	0.52
(c)								
−0.50	0.56	0.53	0.68	0.39	0.86	0.25	0.27	0.96
−0.75	0.37	0.59	0.53	0.30	0.80	0.25	0.25	0.95
−1.00	0.28	0.46	0.50	0.28	0.73	0.16	0.19	0.88
−3.00	0.0	0.15	0.09	0.09	0.20	0.0	0.0	0.41
0.50	0.50	0.59	0.71	0.44	0.86	0.30	0.28	0.95
0.75	0.25	0.37	0.56	0.35	0.80	0.26	0.26	0.93
1.00	0.18	0.37	0.40	0.26	0.76	0.17	0.15	0.84
3.00	0.0	0.09	−0.03	0.07	0.25	0.0	0.0	0.43

up to three watermark attacks. Furthermore, $\text{WW-EMCC}_{\text{N}}$ can achieve higher NC values since the tree group information is the private key during the watermark detection.

3.4 Complexity of WW-EMCC algorithm

The computation complexity of WW-EMCC is low from the view of mathematical analysis. The whole complexity should be discussed for wavelet transform, tree energy sorting and decision calculation respectively.

Suppose the synthesis filters are h (low-pass) and g (high-pass) for wavelet transform. Take $|h|=2N$, $|g|=2M$, and assume $M \geq N$. The cost of the standard algorithm for CDF 9/7 filters is $4(N+M)+2$ and could be speeded up by the lifting algorithm in [12] to $2(N+M+2)$. The computation of wavelet transform is linear time mathematics.

Table 7 Correlation coefficient ρ and watermark existence upon attacks of multiple watermarking with 64bit and 512 bit watermark length. (a) Lena (b) Goldhill (c) Peppers

No.	64 bits			512 bits				
	MWTQ	WW-EMCC		MWTQ	WTGM	WTQ	WW-EMCC	
		Blind	Non-Blind				Blind	Non-Blind
(a)								
1	1.00	0.96	1.00	0.99	0.96	0.65	0.72	1.00
2	0.87	0.87	1.00	0.82	0.86	0.41	0.58	1.00
3	0.75	0.75	1.00	0.71	0.73	0.27	0.45	1.00
4	0.62	0.75	1.00	0.65	0.62	0.11	0.36	1.00
(b)								
1	1.00	0.75	1.00	0.98	0.99	0.79	0.77	1.00
2	0.87	0.59	1.00	0.87	0.86	0.45	0.59	1.00
3	0.75	0.68	1.00	0.78	0.77	0.31	0.48	1.00
4	0.62	0.65	1.00	0.73	0.74	0.18	0.37	1.00
(c)								
1	1.00	0.90	1.00	0.98	0.98	0.80	0.67	1.00
2	0.93	0.78	1.00	0.84	0.84	0.53	0.51	1.00
3	0.84	0.81	1.00	0.77	0.73	0.31	0.41	1.00
4	0.87	0.68	1.00	0.64	0.75	0.22	0.32	1.00

WW-EMCC$_N$ needs the tree energy sorting calculation which can be implemented by quicksort [26] to order the supertrees based on the tree energy to get such an arrangement easily. Therefore, its time complexity requires only about $(2+2\ln 2)R$ comparisons if R items are sorted and the complexity of the quicksort-based selection is linear-time on the average [26].

The watermark decision procedure for $(\beta_k^{'}-\beta_{k+1}^{'})\times(\beta_{k+2}^{'}-\beta_{k+3}^{'})>0$ is pure add, subtract and comparison (there is actually no need to do the real multiplication since the decision is based on the polarity of the multiplication and this can be done in linear time.) From our simulation, the whole loop of WW-EMCC$_N$ embedding and extraction under Intel Pentium 3.2G Hz, 1G RAM desktop computer will need less than 2 seconds to complete for 512×512 testing images. For WW-EMCC$_B$, the speed is even faster since less calculation is needed. In conclusion, the WW-EMCC complexity is low and suitable for practical applications from the mathematical analysis and simulation results.

3.5 Discussion of WW-EMCC$_N$ scheme

Since there are two options (lossy and lossless version) of non-blind watermarking for WW-EMCC$_N$ scheme, it is necessary to investigate their characteristics in order to compare the difference with other techniques. For lossy WW-EMCC$_N$, it is similar to non-blind technique of MWTQ, WTGM and ABW-TME where the cover image is modified for watermark embedding with private key kept secure for the watermark extraction. Therefore, the watermarked image is different from the original image. On the other hand, the outcome of lossless WW-EMCC$_N$ is identical to the original image and the private key includes detailed grouping information which is similar to captioning watermarks mainly used for conveying side information [9]. According to the conveyance of authentication data, it is categorized as labeling-based authentication scheme that store the authentication data in a separate file. Consequently, the authentication data becomes the integral part of the original multimedia and must be transmitted securely [7]. Accordingly, WW-EMCC$_N$ has dual functions: watermark embedding and authentication purposes under our design. However, only one watermark extraction procedure is required for WW-EMCC$_B$ and WW-EMCC$_N$ with different parameters. The simplicity and elegance of WW-EMCC algorithm is also unique which is new for watermarking techniques.

3.6 Human Visual System (HVS) study for WW-EMCC

Where to embed the watermark information in the wavelet domain is very critical for the image quality of watermarked images. The compromise adopted by many DWT-based watermarking algorithms is to embed the watermark in the middle wavelet subbands where acceptable performance of imperceptibility and robustness could be achieved. This is motivated by the following: i) The HVS is sensitive to changes in the lower frequencies as they are associated to the more significant characteristics of the image. Hence embedding watermarks in these areas may degrade the image significantly. ii) The higher frequencies subband coefficients give the details of the image (texture and edges) but changes in the higher frequencies could be easily eliminated through compression and noise attacks. Therefore, the watermark is embedded by modifying the middle frequency coefficients of the host image in order to provide suitable compromise between imperceptibility and robustness [1, 3].

For watermarked images, there has been a need for good metrics for image quality that incorporates properties of the Human Visual System (HVS). The visibility thresholds of visual signals are studied by psychovisual measurements to determine the thresholds. Mannos and Sakrison originally presented a model of the contrast sensitive function (CSF) for luminance (or grayscale) images in [23]. The knowledge from CSF can be used to develop a image independent HVS model. CSF masking [17, 28] is one way to apply the CSF in the discrete wavelet domain. CSF masking refers to the method of weighting the wavelet coefficients according to their perceptual importance. Since WW-EMCC applies the modulation for trees in different wavelet subband, it is an important issue to characterizes the local image properties and identifies texture and edge regions. Future studies can apply the HVS model to determine the optimal watermark locations and strength during the watermark embedding stage which can provide a better visual effect of the watermarked image.

3.7 Summary

In general, WW-EMCC applies the tree difference with positive and negative modulation instead of quantization to embed the watermarks and the cryptanalysis-like attack for WTQ is not useful to remove the watermark for WW-EMCC. From the tabulated results, WW-EMCC is very effective in resisting compression and common signal processing attacks as well as cryptanalysis with comparable performance to MWTQ and WTGM. Especially, the results of WW-EMCC$_N$ are superior to MWTQ and WTGM while the private keys are involved. In summary, WW-EMCC$_N$ is better than WW-EMCC$_B$since global sorting of tree groups with modulation will guarantee the best choice among selections. Besides, non-blind watermarking techniques need to store the secret information which addresses extra storage space and blind watermarking approaches are more practically in use. In the mean time, WW-EMCC$_B$ is the best choice since for the blind watermarking approach since it doesn't need the side information during the watermark extraction.

The extended study should working on the design to efficiently reduce the extra cost with sufficient security for WW-EMCC$_N$. The human visual characteristics can be considered in the wavelet tree based watermarking systems to provide a better visual quality. In addition, WW-EMCC watermarking technique can consider to utilize medium-high frequency wavelet coefficients which have been shown more robust for geometric attack in the study of [30]. Feature-based or other RST (Rotation, Scaling and Translation) invariant mechanisms can be taken into account for better synchronization.

4 Conclusion

An efficient differential energy watermarking algorithm based on wavelet tree group modulation and consistency check has been presented in this study. The employment of wavelet tree structure, grouping selection and bilateral modulation to embed the watermark in the tree group coefficients as well as the relationship between the tree groups effectively improve the robustness of WW-EMCC watermarking. The proposed algorithm improves the disadvantages of WTQ scheme to resist the cryptanalysis attack and it provides flexible options with blind (WW-EMCC$_B$) and non-blind (WW-EMCC$_N$) watermarking techniques. The watermarked images by the proposed technique can resist high degree of signal processing attacks. Intensive studies and large image data set evaluations with other methods like WTQ, MWTQ and WTGM are also compared in this research. For WW-EMCC$_B$, the scheme does not need to store the group ordering information which can reduce the storage space for practical use. In addition, WW-EMCC$_B$ can tolerate many common signal processing and geometric attacks with superior performance than WTQ. Furthermore, if the grouping information is allowed, lossy version of WW-EMCC$_N$ can even provide stronger security strength than MWTQ and WTGM methods. On the other hand, lossless version of WW-EMCC$_N$ performs like a caption based watermarking or digital signature for authentication purpose. Such novel design of WW-EMCC is unique with outstanding performance against attacks.

References

1. Al-Haj A (2007) Combined DWT-DCT digital image watermarking. J Comput Sci 3(9):740–746
2. Al-Otum H-M, Samara N-A (2006) Adaptive blind wavelet-based watermarking technique using tree mutual differences. J Electron Imaging 15(4):043011
3. Amirgholipour SK, Naghsh-Nilchi AR (2009) Robust digital image watermarking based on joint DWT-DCT. JDCTA 3(2):42–54
4. An L, Gao X, Xuelong L, Tao D, Deng C, Li J (2012) Robust reversible watermarking via clustering and enhanced pixel-wise masking. IEEE Trans Image Process 21(8):3598–3611
5. Bender W, Gruhl D, Morimoto N, Lu A (1996) Techniques for data hiding. IBM Syst J 35(3&4):313–336
6. Chan CS, Chang CC, Vo HP (2012) A user-friendly image sharing scheme using JPEG-LS median edge predictor. J Inf Hiding Multimed Signal Process 3(4):340–351
7. Chen T-H, Horng G-B, Lee W-B (2005) A publicly verifiable copyright-proving scheme resistant to malicious attacks. IEEE Trans Ind Electron 52(1):327–334
8. Cox IJ, Leighton FT, Shamoon T (1997) Secure spread spectrum watermarking for multimedia. IEEE Trans Image Process 6(12):1673–1687
9. Cox IJ et al (2007) Digital Watermarking and Steganography, 2nd Ed., Morgan Kaufmann Publishers
10. Das TK, Maitra S, Mitra J (2005) Cryptanalysis of optimal differential energy watermarking (DEW) and a modified robust scheme. IEEE Trans Signal Proc 53(2):768–775
11. Das TK, Mitra S (2006) Analysis of the wavelet tree quantization watermarking strategy and a modified robust scheme. Multimed Syst 12:151–163
12. Daubechies I, Sweldens W (1998) Factoring wavelet transforms into lifting steps. J Fourier Anal Appl 4(3):247–269
13. ECRYPT: http://bows2.ec-lille.fr/index.php?mode=VIEW&tmpl=index1
14. Gao XB, An LL, Yuan Y, Tao DC, Li XL (2011) Lossless data embedding using generalized statistical quantity histogram. IEEE Trans Circ Syst Video Technol 21(8):1061–1070
15. Gao XB, Deng C, Li XL, Tao DC (2010) Geometric distortion insensitive image watermarking in affine covariant regions. IEEE Trans Syst Man Cybern Part C Appl Rev 40(3):278–286
16. Huang HC, Fang WC (2010) Metadata-based image watermarking for copyright protection. Simul Model Pract Theory 18(4):436–445

17. Huang BB, Tang SX (2006) A contrast-sensitive visible watermarking scheme. IEEE Multimed 13(2):60–66
18. JPEG 2000 compression, the International standard (IS 15444–1: JPEG 2000) published from ISO/IEC, [Online]:http://www.ece.uvic.ca/mdadams/hasper/~StirMark, http://www.petitcolas.net/fabien/software/StirMarkBenchmark_4_0_129.zip
19. Kodak Lossless True Color Image Suite: http://www.r0k.us/graphics/kodak/
20. Kundur D, Hatzinakos D (1998) Digital watermarking, using multiresolution wavelet decomposition. Proc IEEE ICASSP 5:2869–2972
21. Langelaar GC, Lagendijk RL (2001) Optimal differential energy watermarking of DCT encoded images and video. IEEE Trans Image Proc 10(1):148–158
22. Lu C-S, Huang S-K, Sze C-J, Liao H-Y (2000) Cocktail watermarking for digital image protection. IEEE Trans Multimed 2(4):209–224
23. Mannos JL, Sakrison DJ (1974) The effects of a visual fidelity criterion on the encoding of images. IEEE Trans Inf Theory 20(4):525–536
24. Podilchuk CI, Zeng W (1998) Image-adaptive watermarking using visual models. IEEE J Sel Areas Commun 16(4):525–539
25. Ritchey PC, Rego VJ (2012) A context sensitive tiling system for information hiding. J Inf Hiding Multimed Signal Process 3(3):212–226
26. Sedgewick R (2001) Algorithms in C, Parts 1–5: fundamentals, data structures, sorting, searching, and graph algorithms, 3rd Edition, Addison Wesley
27. StirMark, http://www.petitcolas.net/fabien/software/StirMarkBenchmark_4_0_129.zip
28. Tsai MJ, Lin CW (2008) Wavelet based multipurpose color image watermarking by using dual watermarks with human vision system models. IEICE E91-A(6)
29. Tsai M-J, Shen C-H (2007) Wavelet tree group modulation (WTGM) for digital image watermarking. IEEE ICASSP 2:173–176
30. Tsai M-J, Shen C-H (2008) Differential energy based watermarking algorithm using Wavelet Tree Group Modulation (WTGM) and human visual system. IEICE Trans Fundam E91-A(8):1961–1973
31. USC-SIPI Image Database: http://sipi.usc.edu/database/
32. Voloshynovskiy S et al (1999) A stochastic approach to content adaptive digital image watermarking. Proc 3rd Int Work Inf Hiding, Dresden, Germany, pp. 211–236
33. Wang S-H, Lin Y-P (2004) Wavelet tree quantization for copyright protection watermarking. IEEE Trans Image Process 13(2):154–165

Min-Jen Tsai received the B.S. degree in electrical engineering from National Taiwan University in 1987, the M.S. degree in industrial engineering and operations research from University of California at Berkeley in 1991, the engineer and Ph.D. degrees in Electrical Engineering from University of California at Los Angeles in 1993 and 1996, respectively. He served as a second lieutenant in Taiwan army from 1987 to 1989. From 1996 to 1997, he was a senior researcher at America Online Inc. In 1997, he joined the institute of information management at the National Chiao Tung University in Taiwan and is currently a full professor. His research interests include multimedia system and applications, digital right management, digital watermarking and authentication, digital forensic, enterprise computing for electronic commerce applications. Dr. Tsai is a member of IEEE, ACM and Eta Kappa Nu.

Jin-Sheng Yin currently Ph.D. student at the institute of information management, National Chiao Tung University.

Imam Yuadi currently Ph.D. student at the institute of information management, National Chiao Tung University.